

Highly structure-sensitive EXAFS spectra from multinuclear Mn model compounds. Ab initio refinement of a diamond-structure of the S₁-state Mn₄CaCl cluster in photosystem II

Y. Komatsuzaki¹, M. Kusunoki¹, K. Hasegawa², T. Ono², T. Noguchi³

¹Department of Physics, Meiji Univ., 1-1-1 Higashimita, Tama-ku, Kawasaki, 214-8571, Japan. Fax 81-44-934-7911, kusunoki@isc.meiji.ac.jp

²Photo-biology Team, Photodyn. Res. Cent., RIKEN, Sendai, 908-0868, Japan.

³Biophys. Chem. Lab., RIKEN, Wako, 351-0198, Japan.

Keywords: EXAFS, photosystem II, S₁-state, manganese cluster, multinuclear, manganese compound

Introduction

Photosystem II (PSII) from plant is a light-dependent enzyme to oxidize water as a universal source of electrons, protons and oxygen molecules in biosphere. The active site of this enzyme contains a tetranuclear Mn cluster together with cofactors, Ca²⁺ and Cl⁻, (Debus) which will be referred to as “Mn₄CaCl cluster”. This cluster makes an open system which catalyzes the water splitting reaction, 2H₂O → 4e⁻+4H⁺+O₂, with a cycle of five intermediates called Kok’s S_i-state, {S_i; i=0,1,2,3,4}, where S₁ is stable in dark, and S₄ is a transient O₂-binding state (Joliot and Kok). Recently, a good PSII crystal from *S. elongatus* was obtained and used to determine the molecular structure of PSII complex at 3.8 Å resolution (A. Zouni et al.). The observed electron density cloud attributable to the Mn cluster and its location in PSII D1 polypeptide were elucidated, although the resolution is still insufficient.

So far, the direct information on the structure of the Mn₄CaCl cluster was provided from observations of the Mn K-edge EXAFS spectra (Yachandra et al, Goerge et al, MacLachlan et al, Dau et al). The EXAFS spectrum due to a Mn ion represents a normalized interference term at the origin in the final state where the outgoing photoelectron wave and a number of scattered waves by surrounding atoms interfere to each other. In a multinuclear Mn cluster, it is a simple average of EXAFS spectra from *m* Mn ions involved, in which the *i*th Mn spectrum “χ_{*i*}” can be ab initio theoretically calculated as a convergent sum of a renormalized single scattering term, which is given by the sum of contributions from all the *N_i* scattering atoms nearby surrounding the *i*th Mn ion (Σ_{*n*=1}^{*N_i*} χ_{*in*}), a double scattering term, which takes the form Σ_{*n*}Σ_{*n'≠n*} χ_{*inn'*}, and the higher multiple scattering terms, which are mostly negligible in the wave number region, *k*={2*m_e*(*E*-*E*₀)}^{1/2} > 3 Å⁻¹ (*E*₀ is the K-edge energy), yielding

$$\chi(k)=m^{-1}\sum_{i=1}^m\chi_i, \quad \chi_i\approx\sum_{n=1}^{N_i}\chi_{in}+\sum_n\sum_{n'\neq n}\chi_{inn'}. \quad (1)$$

Ab initio self-consistent real space multiple-scattering code, FEFF8.10(A.L. Ankudinov et al, J.J. Rehr and R.C. Albers) augmented by eq 1 can be applied to any multinuclear Mn complex if the structure is known. However, if the structure is not entirely known, we are obliged to use the conventional formula in the “grouping-into-a few shells” (GIS) approximation to reduce the number of structure parameters below that of the relevant independent points in the spectrum (E.A. Stern). Unfortunately, however, the GIS approximation may lead to a serious error in most of multinuclear complexes. In two examples of authentic trinuclear and tetranuclear Mn compounds, it will be demonstrated that the interference effect can take place in some groups involving many component waves in {χ_{*in*}; *i*=1-*m*, *n*=1-*N_i*}, sensitively depending upon the effective radial distribution of scattering atoms in each group. As mentioned in *Abstract*, we will present the first refined structure of a diamond-model Mn₄CaCl cluster (M. Kusunoki, S13-008) that is consistent with both EXAFS and X-ray diffraction data.

Materials and Methods

BBY-type PS II membranes prepared from spinach were dark-incubated at 0°C for overnight. The dark-adapted membranes were washed twice with a buffer medium containing 400 mM sucrose, 20 mM NaCl, 0.5 mM Na-EDTA, 20 mM MES/NaOH (pH 6.5), resuspended in the same medium supplemented with 10 mM CaCl₂, then precipitated by centrifugation at 35000×*g* for 40 min. The resulting pellet was directly applied on a plastic sample holder (1 mm in thickness). Manganese K-edge X-ray absorption spectrum of this 100 % S₁-poised sample was measured in fluorescence-mode at 4 K during steady dedicated operation at 300-200 mA and 3 GeV in the Tsukuba Photon Factory BL-12C station equipped with 19 elements Si(Li) solid-state detector (the total count *i_D*). Energy calibration was performed with

use of a sharp pre-edge peak of KMnO₄ solution at 6,543.3 eV, measured by transmission mode with front and rear ionization chambers (i_f , i_r).

The experimental EXAFS spectrum was extracted from the X-ray absorbance data $\mu(E)(\equiv i_p/i_f)$ according to the formula: $\chi = \{\mu(E) - \mu_{bg}(E) - \Delta\mu(E)\} / \Delta\mu(E)$ for $E > E_0 + 50$ eV, with $\Delta\mu(E) = \Delta\mu_0 \exp(2\sigma_f^2 k^2)$ ($\sigma_f^2 \approx 1.8 \times 10^{-4} \text{ \AA}^2$ for thin sample at Mn K-edge), where the background spectrum $\mu_{bg}(E)$ and the K-edge jump $\Delta\mu_0$ were determined by a stepwise least square method as described in (T. Takano and M. Kusunoki). The K-edge threshold E_0 was also optimized to be 6547.0 eV.

We have referred to the Cambridge Structure Data (CSD) to find out X-ray structures of four authentic Mn complexes which EXAFS spectra (exactly speaking, only the radial distribution spectra) have been reported (V.J. DeRose et al). They are $[\text{Mn}^{\text{IV}}_3\text{O}_4\text{Cl}_2(\text{bipy})_2]^{2+}$ (**1**) (N. Auger et al), $[\text{Mn}^{\text{III}}_4\text{O}_2(\text{OAc})_7(\text{bipy})_2]^+$ (**2**) (J.B. Vincent et al), $[\text{Mn}^{\text{III}}_3\text{Mn}^{\text{IV}}\text{O}_3\text{Cl}(\text{OAc})_3(\text{dbm})_3]$ (**3**) (S. Wang et al), and $[\text{Mn}^{\text{III}}_2\text{O}(\text{OAc})_2(\text{tacn})_2]^{2+}$ (**4**) (K. Wieghardt et al).

Ab initio theoretical EXAFS spectra for these compounds and PSII Mn₄CaCl cluster were calculated with use of FEFF8.1 program. The effect of hydrogens on EXAFS was found to increase the amplitude by at most a few percent, and hence was not taken into account in authentic complexes. The structure refinement to fit into the EXAFS radial distribution was manually carried out with use of CAChe and WebLabViewerPro softwares.

Results and Discussions

In **Fig. 1(a)**, we show the experimental EXAFS radial distribution of scattering atoms in the Mn trimer **1** which molecular structure relevant to the EXAFS is depicted in **Fig. 1(d)**. In order to demonstrate that the X-ray diffraction structure of **1** may be too low in the resolution to explain the observed EXAFS spectrum, we calculated a theoretical EXAFS spectrum from it, **Fig. 1(b)**, with use of an ab initio self-consistent real space multiple-scattering code, FEFF8.10 (A.L. Ankudinov et al, J.J. Rehr and R.C. Albers), which is known to be predictable. The result shows a surprising large disagreement with

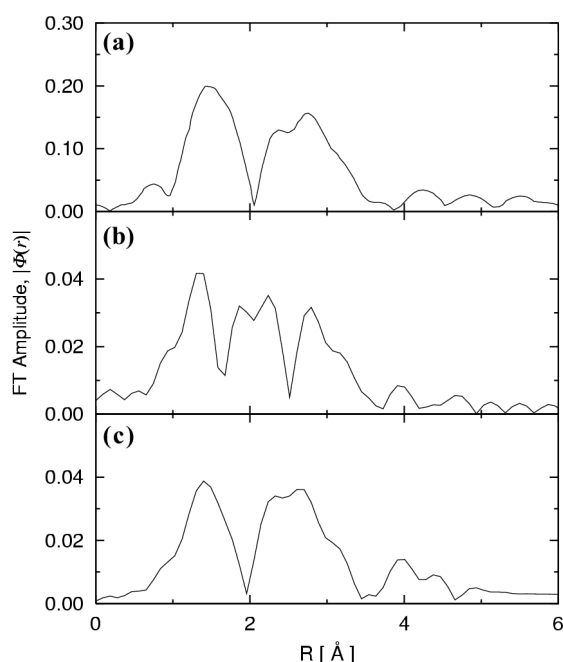
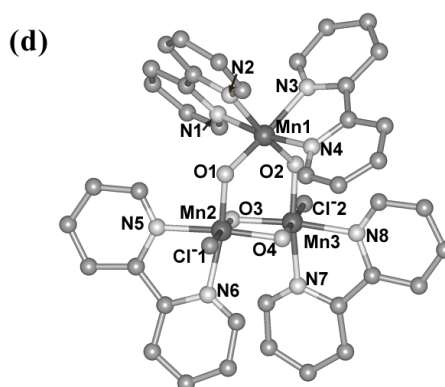


Fig. 1 k^3 -weighted FT amplitudes of the EXAFS spectra for **1**, $\text{Mn}^{\text{IV}}_3\text{O}_4\text{Cl}_2(\text{bipy})_4$: (a) experimental (V. DeRose et al), (b) FEFF8.1 applied to the X-ray diffraction



structure (N. Auger et al) (c) ab initio (FEFF8.1 code) applied to a refined structure (d): the modifications of the relevant bond lengths are shown by arrows in units of \AA ,

$\text{Mn}_1\text{-Mn}_2(3.245 \rightarrow 3.260)$,
 $\text{Mn}_1\text{-Mn}_3(3.241 \rightarrow 3.260)$, $\text{Mn}_2\text{-Mn}_3(2.681 \rightarrow 2.709)$;
 $\text{Mn}_1\{-\text{N}_1(2.020 \rightarrow 2.076), -\text{N}_2(2.107 \rightarrow 2.076), -\text{N}_3(2.100 \rightarrow 2.079),$
 $-\text{N}_4(1.992 \rightarrow 2.077), -\text{O}_1(1.766 \rightarrow 1.842), -\text{O}_2(1.758 \rightarrow 1.837)\}$;
 $\text{Mn}_2\{-\text{O}_1(1.832 \rightarrow 1.837), -\text{O}_3(1.849 \rightarrow 1.930), -\text{O}_4(1.786 \rightarrow 1.929),$
 $-\text{N}_5(2.058 \rightarrow 2.078), -\text{N}_6(2.060 \rightarrow 2.075), -\text{Cl}_1(2.343 \rightarrow 2.470)\}$;
 $\text{Mn}_3\{-\text{O}_2(1.834 \rightarrow 1.840), -\text{O}_3(1.808 \rightarrow 1.930), -\text{O}_4(1.835 \rightarrow 1.931),$
 $-\text{N}_7(2.075 \rightarrow 2.074), -\text{N}_8(2.082 \rightarrow 2.076), -\text{Cl}_2(2.330 \rightarrow 2.450)\}$

experiment (a). This disagreement can not be ascribed to FEFF8.1, because, in the case of the cubane-type tetramer **3**, the experiment and the *ab initio* theory applied to the X-ray structure showed an excellent agreement (data not shown), but, in the X-ray structure of mono- μ_2 -oxo-di- μ_2 -carboxylato bridged dimer **4**, the first-shell peak to be expected was found to be decomposed into three small peaks, although the second peak due to $\sim 2.7 \text{ \AA}$ Mn-Mn bond was predicted at the correct position (data not shown). Hence, we have refined the molecular structure of **1** to get the theoretical spectrum (c) in agreement with spectrum (a). In the **Fig. 1(d)** legend, we have listed the relevant single-scattering pairs with their bond lengths which were manually changed from X-ray structure's (left) to the refined (right) in applications of CAChe and WebLabViewerPro. This refinement includes large increases of order 0.1 \AA in two Mn-Cl bonds and six Mn-O bonds, small increases of order 0.01 \AA in three Mn-Mn bonds and four Mn-O bonds,

and a synchronization of all the Mn-N bonds into 2.074-2.079 Å. This small change resulted in a remarkable change in the spectrum from three peaks to two peaks, which was found to be due to the strong interference effect between EXAFS waves, as mentioned in **Introduction**.

In **Fig. 2(a)**, we show the experimental EXAFS radial distribution of scattering atoms in the adamantine-type manganese tetramer **2** which molecular structure relevant to the EXAFS is depicted in **Fig. 2(d)**. The experimental spectrum **(a)** consists of three intrinsic peaks: the first peak around 1.5 Å would be a result of the superposition of 24 EXAFS waves belonging to the first shell, the second peak around 2.3 Å would have arisen from only one Mn₂-Mn₃ scattering pair with the X-ray bond length of 2.846 Å, and the third peak around 3 Å from four Mn-Mn scattering pairs with the X-ray bond lengths of 3.299-3.384 Å. Surprisingly, however, the theoretical EXAFS spectrum **(b)** based on the *ab initio* code FEFF8.1 was found to be very different from **(a)**, predicting that two well-separated groups of the short and the long Mn-Mn pair waves strongly interfere to each other, yielding a broad band with close merging peaks at ~2.4 and ~2.8 Å. In this region, the multiple scattering terms may critically contribute to this strange nonlinear phenomenon. The refinement of this adamantine structure was very difficult. We report here the best structure refinement we have achieved (see the legend in Fig. 2(d)), which gives the *ab initio* theoretical spectrum **(c)** having similar three peaks to the observed **(a)**. Notably in **(d)**, however, the second peak around 2.3 Å have arisen from one reduced Mn₂-Mn₃ bond of 2.777 Å, and the third peak around 3.2 Å represents an isolated peak of four elongated Mn-Mn bonds, although this elongation appears to be a little bit over. Furthermore, this refinement required large decreases of order 0.1-0.3 Å in 13 Mn-O bonds and large reductions of 7 Mn-O bonds and four Mn-N bonds, all of order 0.1-0.15 Å.

Finally, in Fig.3, we show Mn K-edge EXAFS data from spinach PSII poised in S₁. Dotted wavy lines in panels, (a) and (c), represent the *k*³-weighted EXAFS spectrum, and those in panels, (b) and (d), do the amplitude of the Fourier Transform of this EXAFS spectrum. The *R*-space spectrum in (b, d) exhibits the first shell peak around 1.5 Å and the second shell peak around 2.4 Å, just like the shape repeatedly reported, but do no peak around 3.0 Å, where a weak peak has been observed taking a variety of shape and intensity. Such a missing of 3.0 Å peak may be due to a large background noise that happened to cancel out the signal. Another possibility is that the spectrum around this region is very sensitive to the structure of the Mn₄CaCl cluster, i.e. the sample treatment. In order to demonstrate the latter possibility, and at the same time, to give evidence for the diamond structure model of the Mn₄CaCl cluster, we have studied the structure-dependence of the EXAFS spectrum on this model, which can be incorporated into the real D1 polypeptide. This model cluster contains 2Mn^{III}, 2Mn^{IV}, 1Ca²⁺, 1Cl⁻, 4O²⁻, 1OH⁻, 2His, (2H₂O or OH₂OH⁻), and 6COO⁻, with the total charge of 0 or -1, in S₁-state. For this model, we determined two different structures, designated **L** and **R**: **L** being the best structure that can well simulate our EXAFS

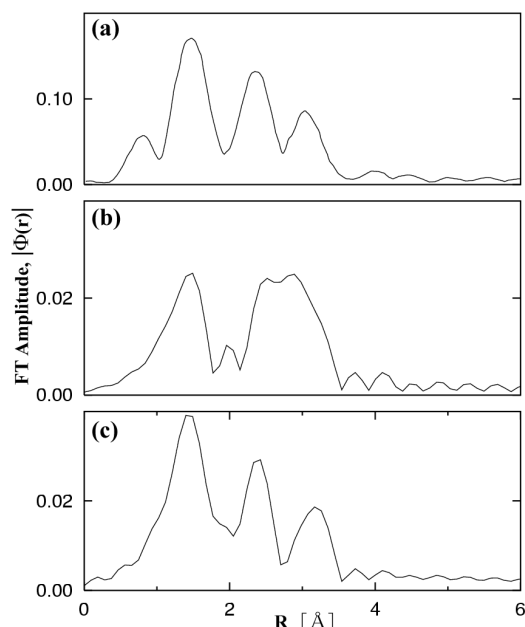
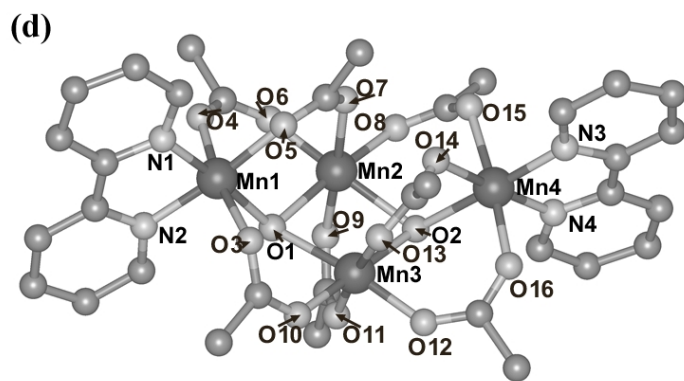


Fig. 2 *k*³-weighted FT amplitudes of the Mn K-edge EXAFS spectra for **2**:Mn^{IV}₃O₄Cl₂(bipy)₄: (a) experimental (V. DeRose et al.), (b) *ab initio* (FEFF8.1 code) applied to the X-ray diffraction structure (J.B. Vincent et al), (c) FEFF8.1 applied to a refined structure (d): the modifications of the



relevant bond lengths are shown by arrows;

Mn₁-Mn₂(3.299→3.539), Mn₁-Mn₃(3.384→3.672),
Mn₂-Mn₃(2.846→2.777), Mn₂-Mn₄(3.370→3.639),
Mn₃-Mn₄(3.311→3.523);
Mn₁{-O₁(1.804→2.136),-O₃(2.172→2.050),-O₄(2.198→1.896),
-O₅(1.915→1.894),-N₁(2.021→1.929),-N₂(2.087→1.929)};
Mn₂{-O₁(1.930→2.099),-O₂(1.887→2.131),-O₆(1.971→1.892),
-O₇(2.260→2.000),-O₈(1.956→1.888),-O₉(2.201→1.899)};
Mn₃{-O₁(1.911→2.126),-O₂(1.919→2.104),-O₁₀(1.937→1.887),
-O₁₁(2.189→1.893),-O₁₂(1.939→1.888),-O₁₃(2.184→1.887)};
Mn₄{-O₂(1.844→2.141),-O₁₄(1.865→2.000),-O₁₅(2.157→2.050),
-O₁₆(2.143→1.903),-N₃(2.077→1.929),-N₄(2.053→1.927)} (Å units).

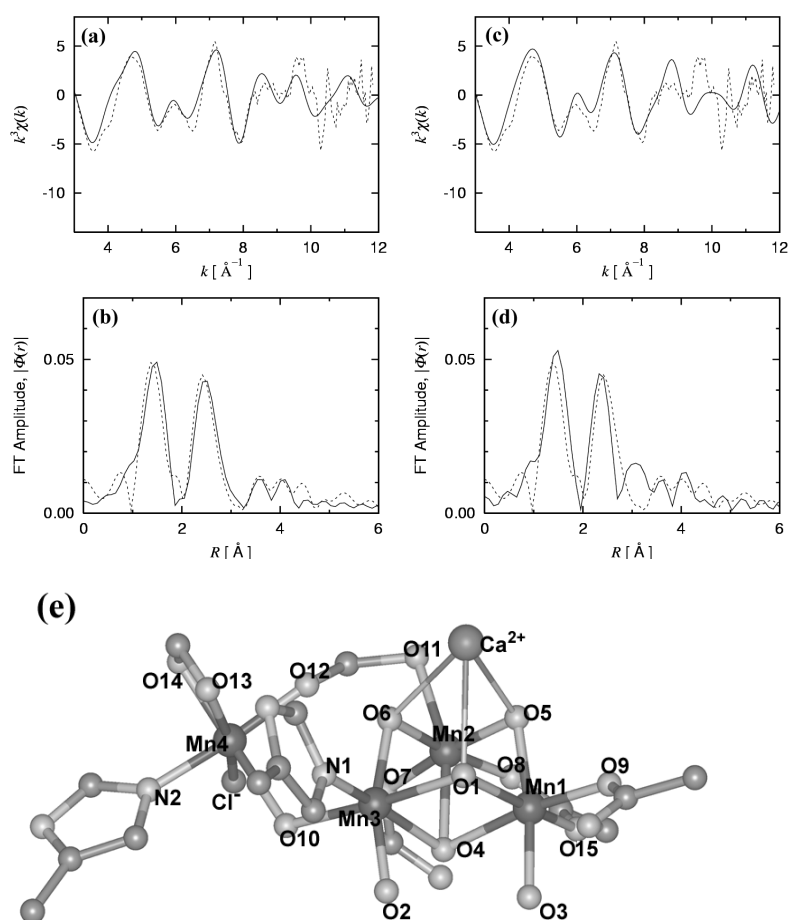


Fig.3 k^3 -weighted Mn K-edge EXAFS data for spinach PSII membranes in S_1 -state: (a,b) the k -space spectrum and (c,d) the R -space spectrum (all, a dotted line). Solid lines in (a,b) and (c,d) represent ab initio theoretical (k,R)-space spectra from slightly different structures, **L** and **R**, of the diamond-type Mn₄CaCl cluster in (e), which are respectively defined by the bond-lengths in the left and right hand sides of slashes in the following:

Mn₁-Mn₂(2.716/2.696),
Mn₁-Mn₃(3.166/3.292),
Mn₂-Mn₃(2.796/2.739),
Mn₂-Mn₄(4.408/4.408),
Mn₃-Mn₄(3.885/3.777);

Mn₁{-O₁(2.178/2.268),
-O₃(1.876/1.855),-O₄(2.108/2.141),-O₅(1.870/1.949),
-O₉(1.879/1.921),-O₁₅(1.868/1.918),-Ca(3.813/3.637)};
Mn₂{-O₄(2.105/2.113),-O₅(1.860/1.932),-O₆(1.909/2.001),
-O₇(1.894/1.894),-O₈(1.886/1.886),-O₁₁(2.119/2.168),-Ca(3.884/3.731)};
Mn₃{-O₁(2.187/2.199),-O₂(2.008/1.872),-O₄(2.129/2.131),
-O₆(1.904/1.987),-O₁₀(2.209/2.121),-N₁(1.924/1.924),-Ca(3.872/3.828)};
Mn₄{-O₁₀(2.218/2.218),-O₁₂(1.832/1.913),-O₁₃(1.928/1.879),
-O₁₄(1.799/1.875),-N₂(1.999/1.922),-Cl(2.157/2.157)}.

data with a missing 3.0Å peak, as seen from **Fig. 3(a,b)**, and **R** to a slightly modified structure that can generate a 3.0 Å peak, as seen from **Fig. 3(c,d)**. Significantly, both of these model structures interpret two small peaks at ~3.6 Å and ~4.1 Å, where Ca is an important scatterer and some multiple scattering terms contribute. The essential difference between **L** and **R** arises from the Mn₁-Mn₃ bond (3.166 Å vs 3.292 Å) which is considered to provide two binding sites of H₂O and/or O₂. Such a small decrease of 0.13 Å could occur depending on the sample treatment. At the end, we emphasize that the 2.4 Å peak can be generated by a 2.716/2.696 Å Mn₁-Mn₂ bond and a 2.796/2.739 Å Mn₂-Mn₃ bond.

Acknowledgements

Thanks are due to the staff of the Photon Factory, especially Prof. S. Nomura, for their assistance (July 1995).

References

- A.L. Ankudinov, B. Ravel, J.J. Rehr and S.D. Conradson (1998) Phys. Rev. B, 7565.
- N. Auger, J.-J. Girerd, M. Corbella, A. Gleizea and J.-L. Zimmermann (1990) J. Am. Chem. Soc. 112, 448-450.
- H. Dau, L. Iuzzolino and J. Dittmer (2001) Biochim. Biophys. Acta 1503, 24-39.
- R.J. Debus (1992) Biochim. Biophys. Acta 1102, 269-352.
- V.J. DeRose, I. Mukerji, M.J. Latimer, V.K. Yachandra, K. Sauer and M.P. Klein (1994) J. Am. Chem. Soc. 116, 5239-5249.
- G. George, R.C. Prince and S.P. Cramer (1989) Science 243, 789-791
- P. Joliot and B. Kok (1975) in *Bioenergetics of Photosynthesis: Oxygen Evolution in Photosynthesis* (Govindjee, ed.) pp. 387-412, Academic Press, New York.
- M. Kusunoki, T. Ono, T. Noguchi, Y. Inoue and H. Oyanagi (1993) Photosynth. Res. 38, 331-339
- M. Kusunoki, T. Takano, T. Ono, T. Noguchi, Y. Yamaguchi, H. Oyanagi and Y. Inoue (1995), in *Photosynthesis: from Light to Biosphere* (P. Mathis, ed.), Vol.II, 251-254, Kluwer Academic Publishers, Dordrecht.
- P.A. Lee, P.H. Citrin, P. Eisenberger and B.M. Kincaid (1981) Rev. Mod. Phys. 53, 769-806
- D.J. MacLachlan, J.H.A. Nugent, P.J. Bratt and M.C.W. Evans (1994) Biochim. Biophys. Acta 1186, 186-200
- J.J. Rehr and R.C. Albers (1990) Phys. Rev. B41, 8139.
- J.B. Vincent, C. Christmas, J.C. Huffman, G. Christou, H.-R. Chang, and D.N. Hendrickson (1987) J. Chem. Soc. Chem. Commun. 236-238.
- T. Takano and M. Kusunoki (2000) Research Report of School of Sci.&Tech. in Meiji Univ. No.22 (78), 17-36.
- S. Wang, K. Folting, W.E. Streib, E.A. Schmitt, J.K. McCusker, D. Hendrickson and G. Christou (1991) 30, 305-306.
- K. Wieghardt, U. Bossek, D. Ventur and J. Weiss (1985) J. Chem. Soc. Chem. Commun. 347-349.